

# Method for employing particle swarm algorithm to design LED collimator system

X. PANG, H. QIN\*

*School of Physics and Optoelectronics Engineering, Shandong University of Technology, Zibo 255000, China*

The comprehensive learning particle swarm optimization technique (CLPSO) is employed to design collimator systems for LED planar light sources, and its fitness function is the merit function of a collimator system which is constructed from sets of light ray displacements and can be obtained from basic geometric-optics analyses. The detailed implementation process is given. A collimator system for a 1 mm diameter round LED consisting of two lenses and a reflector has been designed. The maximum half divergence angle  $\pm 4.6$  degree of exit light rays can be measured from the experiment, which is agreement with the simulation results.

(Received October 29, 2017; accepted February 12, 2019)

*Keywords:* LED, Collimating optical system, CLPSO algorithm

## 1. Introduction

High power LED light sources are in rapid development, as they have higher luminous efficiency, less electricity consumption, longer service life than traditional incandescent lamps. Compared to a fluorescent lamp, they still don't contain mercury and lead, don't emit ultraviolet light, have non-stroboflash. They usually have smaller size, fast response speed and resistance to vibration. Therefore the LED has been widely used in the lighting field. However, the beam emitted by the LED has divergence angles of  $\pm 90$  degree, and often illuminate those areas which do not require light, thus a big deal of light energy can be wasted, even light pollution also comes [1].

It has become a realistic requirement that the beam divergence angle is greatly compressed to transform the beam emitted from LEDs into the nearly parallel beam, such as searchlights, flashlights, night-vision systems, vehicle's headlight, and optical focusing systems and so on. Compressing the divergence angle mainly depends on a collimator system, and the most commonly used LED collimator system usually consists of a freeform surface lens and a curved reflector [2-4]. Designing such a system requires solving a set of differential equations established from the mapping relation between a light source and a target illumination area [2,5-7]. The premise of these methods is that a surface light source is treated as a point source [3,8]. The professional software is used as a simulation tool to simulate the beam from a surface light source passing through the designed system, if the simulation results are not satisfactory, the system will be redesigned. A light intensity distribution on the lighted surface, the maximum half divergence angle and the light energy utilization efficiency are also obtained by the

simulation [9,10]. Literature [3] uses this method to design a collimation system for  $1\text{mm} \times 1\text{mm}$  LED light source, and the system has a light utilization efficiency of 81.5% within a half divergence angle of 5 degree. A system in literature [8] has an efficiency of 86.5% within a half angle of 5 degree. However, the LED is not ideal point source after all, and its actual size cannot be ignored. So this method is not very suitable for secondary LED optical system design. It is necessary to develop a new method of designing a collimator for surface light sources. The PSO algorithm is a global optimization algorithm. Since its advent in 1995, this algorithm has been employed successfully to solve many complex optimization problems, but it has still not been applied in the design of LED collimator systems in the published literatures. Thus, it is a useful attempt to apply the PSO algorithm to design of LED collimator systems, which can not only enrich the design methods of collimator systems, but also promote the development of PSO itself. More importantly, the PSO algorithm can aim directly at the collimation design of surface light sources, which is an important advantage over the mapping method.

This study presents a straightforward method for designing a collimator system for a LED planar light source. In this method, a merit function for beam collimation is constructed based on the analysis of refraction and reflection, the CLPSO algorithm are employed to find the smallest merit function value of the best possible solution. This method neither requires solving complex differential equations nor fitting curves or surfaces from discrete points [11]. As an example of using this method, a collimator system which can compress a beam from a round LED of diameter 1 mm within a half divergence angle of 4.6 degree is given. The paper shows

the theoretical foundation and the rationality of this method, and verifies design results with collimating lenses.

## 2. Optical Structure of LED collimator and problem identification

### 2.1. The basic structure of the collimator system

The traditional LED collimator usually consists of a collimating lens and a curved reflector, and the divergence angle of an output beam is mainly brought about by a collimating lens. In order to further reduce the divergence angle, two collimating lenses will be used in this paper. Fig. 1 shows a section profile of a fundamental structure of a LED collimator. This is a rotational symmetric system, consisting of a curved reflector, a meniscus lens and a bi-convex lens. A round LED with 1 mm diameter (central wavelength 520 nm) is placed at location 1. The rays emitted by the LED transport through the two lenses if they are within a circle whose diameter is  $P_1P_2$  in Fig. 1, otherwise they are reflected by the reflector. Here, a circular hole of diameter  $P_1P_2$  may be considered the virtual aperture of collimating lenses.

A meniscus lens and a bi-convex lens belong to the spherical lenses, their radius and height are part of design optimization, and the axial distances between neighboring spherical surfaces must also be part of design optimization. The reflector in Fig. 1 was set as an aspheric surface with even order:

$$x = d + \frac{Ch^2}{1 + \sqrt{1 - h^2C^2(1 + a_2)}} + a_4h^4 + a_6h^6 + a_8h^8 \quad (1)$$

where  $h = \sqrt{y^2 + z^2}$ ,  $a_2, a_4, a_6, a_8$  are coefficients,  $C$  is the curvature of the second order surface at apex and  $d$  is the distance between the coordinate origin and the apex of this aspheric surface.

In the below section, we will respectively analyze the reflecting characteristics of an aspheric surface and the refraction characteristics of collimating lenses, and whereby the design method for collimating lenses and a reflecting surface is found.

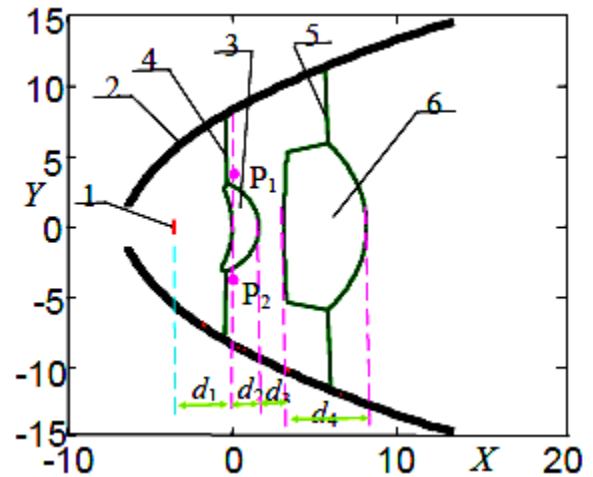


Fig. 1. The structure of the proposed LED collimator. 1-LED source; 2-Reflector; 3- Meniscus lens; 4- Transparent plate fixing meniscus lens; 5- Transparent plate fixing Bi-convex lens; 6-Bi-convex lens

### 2.2. The analysis on a reflecting surface

Fig. 2 shows rays reflected from the reflector with Cartesian coordinate.  $P_0(x_0, y_0, z_0)$  is an arbitrary point on the LED source. The LED divergence angle is set between  $-85^\circ$  and  $85^\circ$  in the design process, thus  $P_0$  point has the same divergence angle. Only these rays within a  $P_1P_2$  diameter circle can pass through the meniscus lens and the bi-convex lens. Otherwise, light rays will irradiate on the reflecting surface outside the system. Let the coordinates of point  $P_1$  be  $(0, h_{\max}, 0)$ , then the rays being within  $\tan^{-1}(\frac{h_{\max} - y_0}{x_0}) \leq \theta \leq 85^\circ$  and  $-85^\circ \leq \theta \leq \tan^{-1}(\frac{-h_{\max} - y_0}{x_0})$  will irradiate on the reflecting surface. Take any a light ray in above intervals, the angle between this ray and the horizontal line through point  $P_0$  is  $\theta_k$ . Set  $\vec{Q}_1(\alpha_1, \beta_1, \gamma_1)$  to be the unit ray vector of this incident ray, and it can be calculated from an angle  $\theta_k$ . The intersection point  $P(x, y, z)$  between this incident ray and an aspheric surface is then calculated by a published method [12]. The normal unit vector  $\vec{N}(\alpha_N, \beta_N, \gamma_N)$  at  $P(x, y, z)$  can be obtained from the coordinate of point  $P$  and Eq.(1). The unit ray vector of the reflected ray at the point  $P$  is represented by  $\vec{Q}_2(\alpha_2, \beta_2, \gamma_2)$ , and it can be got from the

vectorial law of reflection:

$$\bar{Q}_2 = \bar{Q}_1 - 2(\bar{Q}_1 \cdot \bar{N})\bar{N} \quad (2a)$$

The component expression of the above equation is:

$$\begin{cases} \alpha_2 = \alpha_1 - 2(\bar{Q}_1 \cdot \bar{N})\alpha_N \\ \beta_2 = \beta_1 - 2(\bar{Q}_1 \cdot \bar{N})\beta_N \\ \gamma_2 = \gamma_1 - 2(\bar{Q}_1 \cdot \bar{N})\gamma_N \end{cases} \quad (2b)$$

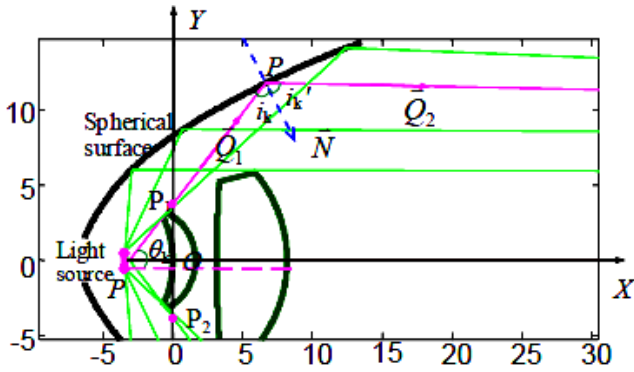


Fig. 2. The rays reflected by the reflecting surface of the collimating system

If the reflected ray at a point P exits along the direction of  $\bar{Q}_2$ , then it has a projection on the Y axis,  $\Delta y = (\beta_2 / \alpha_2) \Delta x$ , and a projection on the Z axis,  $\Delta z = (\gamma_2 / \alpha_2) \Delta x$ , where  $\Delta x$  is the distance that the reflected ray travels on the X axis. If  $\Delta y = 0$  and  $\Delta z = 0$ , the reflected ray would be parallel to the X axis. Many reflected rays, such as k, can be selected and all these rays give:

$$\sum_k (\Delta y_k^2 + \Delta z_k^2) = \sum_k \left\{ \left[ (\beta_{2,k} / \alpha_{2,k}) \Delta x_k \right]^2 + \left[ (\gamma_{2,k} / \alpha_{2,k}) \Delta x_k \right]^2 \right\} \quad (3)$$

$\Delta x_k$  can be manipulated to be the same for all the rays, then  $\sum_k (\Delta y_k^2 + \Delta z_k^2)$  is only a function of  $\bar{Q}_2$ .

Equation (2) tells that  $\bar{Q}_2$  is a function of incident vector

$\bar{Q}_1$  and normal vector  $\bar{N}$ . However  $\bar{N}$  is a function of the parameters of an aspheric surface  $C, d, a_2, a_4, a_4, a_8$ . If  $\bar{Q}_1$  is fixed,  $\bar{Q}_2$  is only a function of the parameters of the aspheric surface, and eventually  $\sum_k (\Delta y_k^2 + \Delta z_k^2)$  is only a function of the parameters of the aspheric surface  $C, d, a_2, a_4, a_4, a_8$ .

We used  $\sum_k (\Delta y_k^2 + \Delta z_k^2)$  as a fitness function of CLPSO to seek the aspheric parameters with the smallest fitness function value to achieve the purpose of compressing a divergence angle of the LED.

### 2.3. The analysis on a refracting surface

For the two refracting lenses in the LED collimator, we applied same equation (1) for each surface while we set  $a_2 = a_4 = a_6 = a_8 = 0$  to make them spherical surfaces. When rays from any point  $P_0(x_0, y_0, z_0)$  of an LED light source irradiate within a  $P_1P_2$  diameter circle, they will be refracted out of the meniscus lens and the bi-convex lens. Any ray from point  $P_0(x_0, y_0, z_0)$ , passing through a point P  $(0, y_1, z_1)$  within the virtual aperture, gives an incident ray unit vector  $\bar{Q}_1(\alpha_1, \beta_1, \gamma_1)$ :

$$\begin{cases} \alpha_1 = \frac{-x_0}{\sqrt{x_0^2 + (y_1 - y_0)^2 + (z_1 - z_0)^2}} \\ \beta_1 = \frac{y_1 - y_0}{\sqrt{x_0^2 + (y_1 - y_0)^2 + (z_1 - z_0)^2}} \\ \gamma_1 = \frac{z_1 - z_0}{\sqrt{x_0^2 + (y_1 - y_0)^2 + (z_1 - z_0)^2}} \end{cases}$$

The intersection of the incident ray with the first surface of the meniscus lens, together with the normal vector  $\bar{N}(\alpha_N, \beta_N, \gamma_N)$ , can be calculated using same procedure described in the part of reflector design. The refracted ray  $\bar{Q}_2(\alpha_2, \beta_2, \gamma_2)$  can be calculated using the

refraction law  $n\bar{Q}_1 \times \bar{N} = n'\bar{Q}_2 \times \bar{N}$  :

$$\bar{Q}_2 = \frac{n}{n'}\bar{Q}_1 + \frac{g}{n'}\bar{N} \quad (4)$$

with three components:  $\alpha_2 = \frac{n}{n'}\alpha_1 + \frac{g}{n'}\alpha_N$  ,

$$\beta_2 = \frac{n}{n'}\beta_1 + \frac{g}{n'}\beta_N, \quad \gamma_2 = \frac{n}{n'}\gamma_1 + \frac{g}{n'}\gamma_N$$

where  $g = n' \cos I'' - n \cos I$  ,  $I$  and  $I''$  are the incident angle and refracted angle respectively,  $\cos I = |\bar{Q}_1 \cdot \bar{N}| = |\alpha_1\alpha_N + \beta_1\beta_N + \gamma_1\gamma_N|$  ,

$$\cos I'' = \sqrt{1 - n^2/n'^2(1 - \cos^2 I)} .$$

For the 4 surfaces of the two lenses, the above procedure is iterated, the direction vectors  $\bar{Q}_{j+1}(\alpha_{j+1}, \beta_{j+1}, \gamma_{j+1})$  of rays coming out from the each refractive surface will be calculated successively, here  $j$  represents the  $j$ -th refractive surface, in this paper  $j=1,2,3,4$ . Assuming that a ray exiting from the last refractive surface travels a distance, and its projection on the  $X$  axis is  $\Delta x$  , then its projection on the  $Y$  axis,  $\Delta y = (\beta_{j+1} / \alpha_{j+1})\Delta x$  ,  $\Delta z = (\gamma_{j+1} / \alpha_{j+1})\Delta x$  on the  $Z$  axis. If  $\Delta y = 0$  and  $\Delta z = 0$  , then the refracted light will parallel to the  $X$  axis. If enough incident rays are taken, every corresponding refracted ray has  $\Delta y_k$  and  $\Delta z_k$  , where subscript  $k$  denotes the  $k$ -th ray. The sum of  $\Delta y_k^2 + \Delta z_k^2$  of all rays is

$$\sum_k (\Delta y_k^2 + \Delta z_k^2) = \sum_k \left\{ \left[ (\beta_{j+1,k} / \alpha_{j+1,k}) \Delta x_k \right]^2 + \left[ (\gamma_{j+1,k} / \alpha_{j+1,k}) \Delta x_k \right]^2 \right\} \quad (5)$$

Let  $\Delta x_k$  be a constant, then  $\sum_k (\Delta y_k^2 + \Delta z_k^2)$  is only a function of  $\bar{Q}_{j+1}$  . As the analysis of section 2.2,  $\bar{Q}_{j+1}$  is a

function of  $\bar{Q}_j$  and the  $j$ -th aspheric surface parameters

$C, d, a_2, a_4, a_6, a_8$  , and the like, if  $\bar{Q}_1$  is fixed,

eventually  $\bar{Q}_{j+1}$  is only a function of all refractive

aspheric surface parameters, then  $\sum_k (\Delta y_k^2 + \Delta z_k^2)$  is also

just a function of all refractive aspheric surface parameters.

$\sum_k (\Delta y_k^2 + \Delta z_k^2)$  is taken as a merit function for

optimizing aspheric surface parameters.

When  $\sum_k (\Delta y_k^2 + \Delta z_k^2)$  reaches a minimum value, the

divergence angle of the outgoing light from the collimator system will reach a minimum value.

### 3. Optimization procedure – CLPSO [13]

The above analysis shows that the merit function

$\sum_k (\Delta y_k^2 + \Delta z_k^2)$  is a function of the aspheric coefficients,

namely, 
$$\sum_k (\Delta y_k^2 + \Delta z_k^2) = f(C^1, d^1, a_2^1, a_4^1, a_6^1, a_8^1, \dots, C^j, d^j, a_2^j, a_4^j, a_6^j, a_8^j)$$

$j=1,2,3,4$  is the sequence number of refractive surfaces.

For example,  $j=2$  indicates the second refractive surface.

These aspheric parameters with the smallest

$\sum_k (\Delta y_k^2 + \Delta z_k^2)$  are what designers need to pursue.

Therefore the problem becomes one of identifying a mathematical solution of

$$\min \left\{ f(C^1, d^1, a_2^1, a_4^1, a_6^1, a_8^1, \dots, C^j, d^j, a_2^j, a_4^j, a_6^j, a_8^j) \right\} .$$

The CLPSO algorithm is employed to seek the solution to this problem, and a fitness function of CLPSO is

$$\sum_k (\Delta y_k^2 + \Delta z_k^2) \text{ mentioned above.}$$

In the CLPSO algorithm, a feasible solution to the problem

$$\min \left\{ f(C^1, d^1, a_2^1, a_4^1, a_6^1, a_8^1, \dots, C^j, d^j, a_2^j, a_4^j, a_6^j, a_8^j) \right\}$$

is called a particle, a set of feasible solutions is called a swarm, and the number of particles in a swarm is referred

as a particle size (ps). The position of the  $i$ -th particle is represented by a  $D$ -dimensional vector

$$\mathbf{X}_i = (X_i^1, X_i^2, \dots, X_i^D) \quad . \text{ Therefore,} \\ = (C^1, d^1, a_2^1, a_4^1, a_6^1, a_8^1, \dots, C^j, d^j, a_2^j, a_4^j, a_6^j, a_8^j)$$

each allowed particle's position is a solution to the problem, and the optimization process is to seek a particle's position with the the minimum fitness function value, i.e.  $\min\{f(\mathbf{X}_i)\}$ . The velocity of the  $i$ -th particle is expressed as

$$\mathbf{V}_i = (V_i^1, V_i^2, \dots, V_i^D) = \\ (V_{C^1}, V_{d^1}, V_{a_2^1}, V_{a_4^1}, V_{a_6^1}, V_{a_8^1}, \dots, V_{C^j}, V_{d^j}, V_{a_2^j}, V_{a_4^j}, V_{a_6^j}, V_{a_8^j})$$

The refractive and reflective parts of LED collimator are designed respectively, and the design principle is the same. There is only one reflecting surface, so  $j=1$ ,

$$\mathbf{X}_i = (X_i^1, X_i^2, \dots, X_i^D) = (C^1, d^1, a_2^1, a_4^1, a_6^1, a_8^1),$$

$D=6$ . When we optimize the reflecting surface, the dimension of the position space of a particle is 6. The refractive part in the middle of the system consists of two lenses with four refracting surfaces, assuming all four refractive surfaces are aspheric, then  $j = 1, 2, 3, 4$ ,

$$\mathbf{X}_i = (X_i^1, X_i^2, \dots, X_i^D) \\ = (C^1, d^1, a_2^1, a_4^1, a_6^1, a_8^1, \dots, C^4, d^4, a_2^4, a_4^4, a_6^4, a_8^4)$$

$D=24$ . So when we optimize these refracting surfaces, the dimension of a particle's position space is 24. In the following section, we will describe the design process by taking the refractive part as an example.

According to Eqs. (1) - (5),  $\sum_k (\Delta y_k^2 + \Delta z_k^2)$  can be

calculated from the position vector  $\mathbf{X}_i$  of the  $i$ -th particle.

If one or several of four surfaces is spherical, then the corresponding surface's  $a_2^j = a_4^j = a_6^j = a_8^j = 0$ , the dimension of a particle's position space also reduced accordingly, which means the dimension of searching space will be reduced. The below is a brief description of the implementation process of the CLPSO:

(1) Define the search scope of each dimension of the search space, namely, the maximum and the minimum of  $C^j, d^j, a_2^j, a_4^j, a_6^j, a_8^j$ , represented with

$$C_{\max}^j, d_{\max}^j, a_{2\max}^j, a_{4\max}^j, a_{6\max}^j, a_{8\max}^j \quad \text{and}$$

$C_{\min}^j, d_{\min}^j, a_{2\min}^j, a_{4\min}^j, a_{6\min}^j, a_{8\min}^j$ , which are arbitrarily set within a reasonable range according to the actual situation.

(2) Initialize  $\mathbf{X}_i$

$$\mathbf{X}_i = (X_i^1, X_i^2, \dots, X_i^{24}) = \\ (C^1, d^1, a_2^1, a_4^1, a_6^1, a_8^1, \dots, C^4, d^4, a_2^4, a_4^4, a_6^4, a_8^4)$$

The initial value of each dimension of  $\mathbf{X}_i$  is a

random number between its maximum and minimum. For

example,  $X_i^1 = C^1$  is a random number in the interval

$[C_{\min}^1, C_{\max}^1]$ ,  $X_i^3 = a_2^1$  is a random number in the interval

$[a_{2\min}^1, a_{2\max}^1]$ , and so on.

(3) Initialize  $\mathbf{V}_i$

$$\mathbf{V}_i = (V_i^1, V_i^2, \dots, V_i^{24}) = \\ (V_{C^1}, V_{d^1}, V_{a_2^1}, V_{a_4^1}, V_{a_6^1}, V_{a_8^1}, \dots, V_{C^4}, V_{d^4}, V_{a_2^4}, V_{a_4^4}, V_{a_6^4}, V_{a_8^4})$$

The initial value of each dimension of  $\mathbf{V}_i$  is a random

number within its maximum and minimum. For example,

$V_i^1 = V_{C^1}$  is a random number in the interval

$[V_{C^1\min}, V_{C^1\max}]$ , and  $V_i^3 = V_{a_2^1}$  is a random number in

the interval  $[V_{a_2^1\min}, V_{a_2^1\max}]$ . In general,

$$V_{C^1\max} = C_{\max}^1 - C_{\min}^1, \quad V_{C^1\min} = -V_{C^1\max},$$

$$V_{a_2^1\max} = a_{2\max}^1 - a_{2\min}^1, \quad V_{a_2^1\min} = -V_{a_2^1\max}, \quad \text{and so}$$

forth.

(4) Initialize the individual best position and the global best position of a swarm. According to Eqs. (1) -

(5),  $\sum_k (\Delta y_k^2 + \Delta z_k^2)$  of each particle in a swarm can be

calculated from the initial value of vector  $\mathbf{X}_i$ , thus, the initial best position  $\mathbf{pbest}_i = (pbest_i^1, pbest_i^2, \dots, pbest_i^D)$  of an

individual particle and one of the swarm  $gbest=(gbest^1, gbest^2, \dots, gbest^D)$  can be obtained. The initial best position of individual particle is the particle's initial position itself, and the initial best position of a swarm is one whose  $\sum_k (\Delta y_k^2 + \Delta z_k^2)$  is the smallest in the swarm.

(5) The  $i$ -th particle updates its velocity and position of  $d$ -th dimension with the following equations [13]:

$$V_i^d \leftarrow \omega * V_i^d + c_1 * rand1_i^d * (1 - ai_i^d) * (pbest_{f_i^d}^d - X_i^d) + c_2 * rand2_i^d * ai_i^d * (gbest^d - X_i^d) \quad (6)$$

$$X_i^d \leftarrow X_i^d + V_i^d \quad (7)$$

where,  $\omega = 0.9 - 0.7 * iter / iter_{max}$ , is the inertia weight,  $iter$  is the current iteration number, and  $iter_{max}$  is the maximum number of iterations. A larger inertia weight is more beneficial to global search, and a smaller inertia weight is suitable for local search, Shi and Eberhart proposed that inertia weight was linearly reduced over the search course [14]. Firstly its value is initialized to 0.9, and then is linearly reduced to 0.2 with an increasing iterations [15].  $c_1$  and  $c_2$  are acceleration constants, let  $c_1 = c_2 = 1.49445$  [16], and they determine random accelerated weights which pull each particle toward the its best position and the swarm's best position, respectively.  $rand1_i^d$  and  $rand2_i^d$  are arbitrary random numbers in the interval [0,1];  $ai_i^d$  is randomly chosen between 0 and 1, it reflects the learning probability from its  $gbest$ , and occupies the half of learning opportunities,  $(1 - ai_i^d)$  is the probability which each particle learns from the  $pbest_i$ ,

and also occupies the half of learning opportunities.

$f_i = [f_i^1, f_i^2, \dots, f_i^D]$  defines which particle's  $pbest_i$  the particle should follow when this particle updates its velocity in the  $d$ th dimension [13].  $pbest_{f_i^d}^d$  can be any particle's  $pbest$  including its own  $pbest$ , the flow chart generating  $f_i$  is shown in Fig. 3, which is rewritten from literature [13].

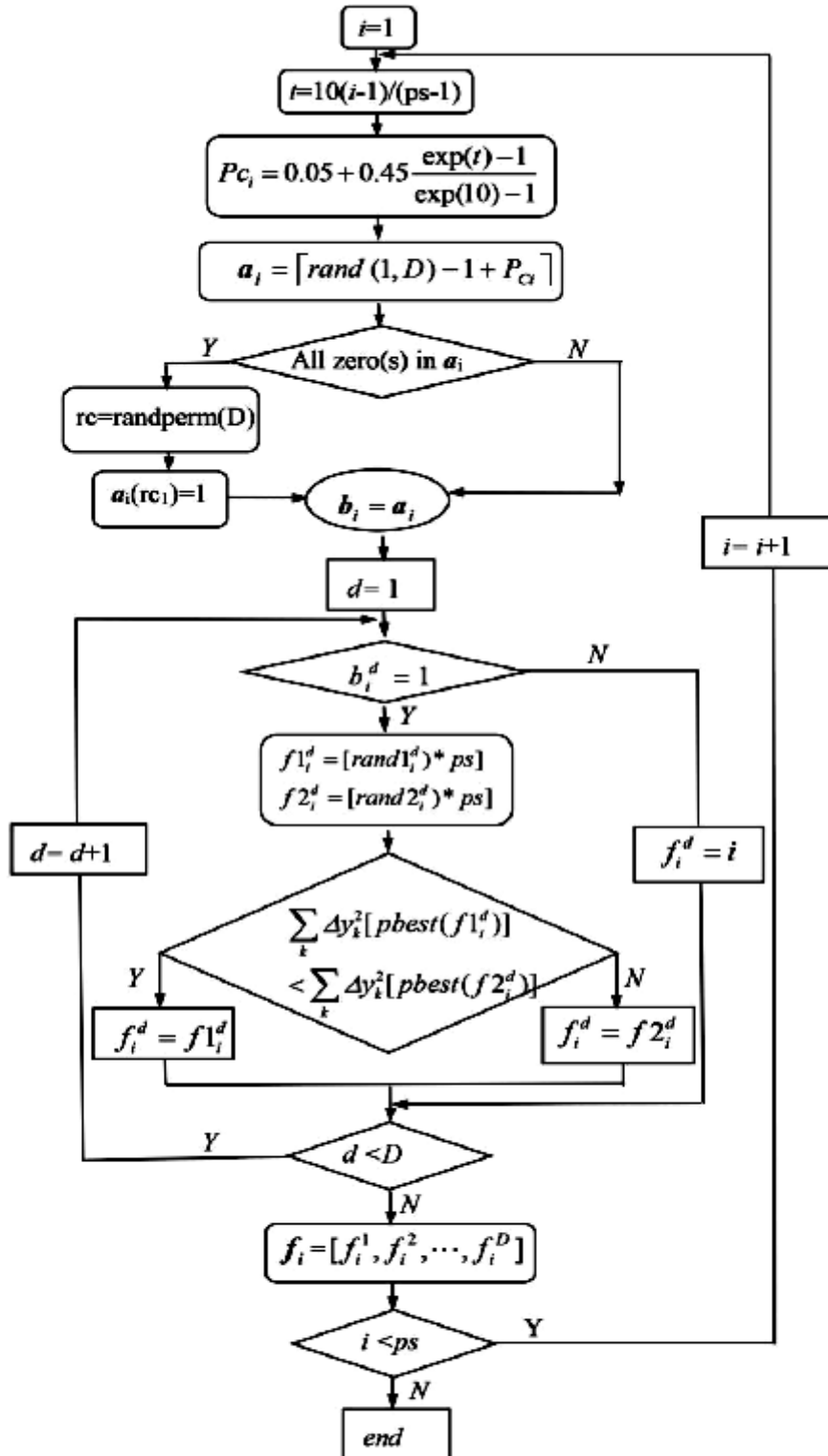
$$(6) \text{ Recalculate } \sum_k (\Delta y_k^2 + \Delta z_k^2) \text{ of each particle}$$

from a new position  $X_i$  of the updated particle according to Eq. (1) - (5), then the individual's new historical best position  $pbest_i$  and the swarm's new historical best position  $gbest$  can be obtained.

(7) Go back to step (5) and (6), and repeat the above steps until the end of the iteration, then the swarm's best position  $gbest$  at the maximum number of iterations is what we look for, it is also structure parameters  $C^j, d^j, a_2^j, a_4^j, a_6^j, a_8^j$  of each refractive surface. From the optimized results, we also get the maximum divergence angle and the location of outgoing light rays.

#### 4. The design example of an LED collimator

This section gives a design example using the above method and ray tracing simulation of collimator systems. K9 glass is selected as lens materials whose refractive index  $n=1.5168$  at center wavelength 520 nm, and both vertical and horizontal dimensions of collimators are required to be less than 30 mm.



$\lceil \cdot \rceil$ : Ceiling operator;  $ps$ : population size;  $i$ : particle's id counter from 1 to  $ps$ ;  
 $D$ : the dimension of the search space;  $d$ : dimension;  $\text{rand}(1,D)$ : returns an 1-by- $D$  matrix;  
 $\text{rand}1_i^d$  and  $\text{rand}2_i^d$ : two random numbers in the range  $[0, 1]$ ;  
 $\text{randperm}(D)$ : returns a random permutation of the integers  $1:n$ ;  
 $\text{rc}=[rc_1, rc_2, \dots, rc_D]$ ;  $\mathbf{a}_i=[a_i(1), a_i(2), \dots, a_i(D)]$ ;  $\mathbf{b}_i=[b_i^1, b_i^2, \dots, b_i^D]$

Fig. 3. The flow chart generating  $f_i$  of the  $i$ th particle

#### 4.1. The design

Assume that a planar light source is a 1 mm diameter round LED, and its center is located at  $(-3.5, 0, 0)$ . It is discretized into the combination of ideal point light sources, then the coordinate of any luminous point on the LED can be expressed as  $P_0(-3.5, y_0, z_0)$ , as shown in Fig. 4.  $P_1P_2$  and  $P'_1P'_2$  can be considered virtual apertures, where  $P_1P_2=2 \times 3.5 \tan(45^\circ)$  and  $P'_1P'_2=2 \times 3.5 \tan(85^\circ)+1$ . The light emitted from the LED is divided into two parts by  $P_1P_2$ , the light passing outside  $P_1P_2$  is incident on the reflecting surface of a collimator, and the light passing between  $P_1$  and  $P_2$  is incident on the lenses in the middle of a collimator.

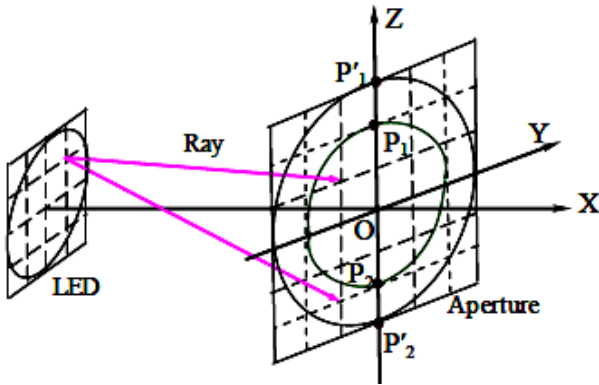


Fig. 4. LED and the aperture are uniformly gridded to regularly select light rays

LED and the aperture are uniformly gridded. A  $1\text{mm} \times 1\text{mm}$  square including a LED is divided into  $(m_1-1) \times (m_1-1)$  grids and has  $m_1 \times m_1$  grid nodes. A square of side length  $P'_1P'_2$  in the aperture plane is divided into  $(m_2-1) \times (m_2-1)$  grids and has  $m_2 \times m_2$  grid nodes. Assume that each grid node on the LED is a point light source whose light is uniformly incident on the aperture, and each point source emits  $m_2 \times m_2$  rays being incident on the each nodes of the aperture respectively. In our program, we set a loop condition, when grid nodes are within this round LED, the loop continues, otherwise the loop stops. We also set such a loop condition for grid nodes on the aperture, when grid nodes are within the  $P_1P_2$  diameter circle, the rays through these nodes will be refracted by two lenses, when grid nodes are outside the  $P_1P_2$  diameter circle but within the  $P'_1P'_2$  diameter circle, the rays through these nodes will be reflected by the reflecting surface.

According to the above analysis, let  $P_1=(0, 3.5, 0)$ ,  $P_2=(0, -3.5, 0)$ ,  $P'_1=(0, 40.5, 0)$ ,  $P'_2=(0, -40.5, 0)$ . Aspheric coefficients of the reflective and refractive surfaces are optimized respectively. Let all four surfaces of two lenses be spherical, then aspheric coefficients in Eq. (1) describing four surfaces  $a_2 = a_4 = a_6 = a_8 = 0$ . Take  $m_1=4$ ,  $m_2=5$ .  $\bar{Q}_1$  of each light ray can be calculated from the nodal coordinates on the LED and ones on the aperture.

First of all, according to step (1) of the CLPSO, the searching ranges of aspheric coefficients for the reflector outside the collimator is defined in Table 1, and the searching ranges of spherical coefficients for four surfaces of two lenses is defined in Table 2. Of course, if the ideal solution can't be found in these search ranges, we can change the search range again.

In the second step of the CLPSO, we wrote a Matlab program according to the implementation process (1)-(7).

With  $\sum_k (\Delta y_k^2 + \Delta z_k^2)$  as the fitness function in CLPSO,

the parameters in Table 1 and Table 2 are optimized respectively; The program runs for about 20 minutes on an intel (R) Core (TM) i5-2300 cpu @2.8GHz processor with 4GB of RAM, and the results are shown in Table 3 and Table 4.

As illustrated in Fig. 1,  $d_1=3.5$  mm,  $d_2=1.635$  mm,  $d_3=1.527$  mm,  $d_4=5.00$  mm can be obtained from Table 4.

The maximum half divergence angles of rays exited from the reflector and collimating lenses are also obtained from the optimization results, and they are 2.19 degree and 4.6 degree, respectively. Therefore, the divergence angle of LED lights after the collimating system is mainly caused by collimating lenses. Fig. 5 shows a three-dimensional structure of the collimator system drawn from parameter data in Table 3 and Table 4.

#### 4.2. The ray-tracing simulation of LED lights passing through the collimator system

Fig. 6 shows the 2D optical path simulation of LED lights through the collimator system determined by the coefficients in Table 3 and Table 4. In Fig. 6, the red line represents the reflected light ray, and the blue line represents the refracted light ray. It can be seen that the reflected light does not pass through collimating lenses in the middle of the collimator system.

Table 1. The search ranges of aspheric parameters for the reflector outside the collimator

$C(1/\text{mm})$	$d(\text{mm})$	$a_2$	$a_4$	$a_6$	$a_8$
[1/50,1/0.5]	[-20,-6]	[-20,0]	$[-8 \times 10^{-3}, 8 \times 10^{-3}]$	$[-8 \times 10^{-6}, 8 \times 10^{-6}]$	$[-8 \times 10^{-9}, 8 \times 10^{-9}]$

Table 2. The search ranges of spherical parameters for front and rear surfaces of a meniscus lens and a biconvex lens

$C^1(1/\text{mm})$	$d^1(\text{mm})$	$C^2(1/\text{mm})$	$d^2(\text{mm})$	$C^3(1/\text{mm})$	$d^3(\text{mm})$	$C^4(1/\text{mm})$	$d^4(\text{mm})$
[-1/3,-1/20]	[0,0]	[-1/2,-1/15]	[0.5,3]	[1/100,1/10]	[2.5,4]	[-1/5,-1/20]	[4.5,9]

Table 3. The optimization result of aspheric parameters for the reflector outside the collimator

$C(1/\text{mm})$	$d(\text{mm})$	$a_2$	$a_4$	$a_6$	$a_8$
0.3409	-6.6387	-3.2623	$6.8831 \times 10^{-4}$	$-3.4307 \times 10^{-6}$	$6.6600 \times 10^{-9}$

Table 4. The optimization result of spherical parameters for front and rear surfaces of a meniscus lens and a biconvex lens

$C^1(1/\text{mm})$	$d^1(\text{mm})$	$C^2(1/\text{mm})$	$d^2(\text{mm})$	$C^3(1/\text{mm})$	$d^3(\text{mm})$	$C^4(1/\text{mm})$	$d^4(\text{mm})$
-0.153453	0	-0.289433	1.635	0.011218	3.162	-0.116486	8.162

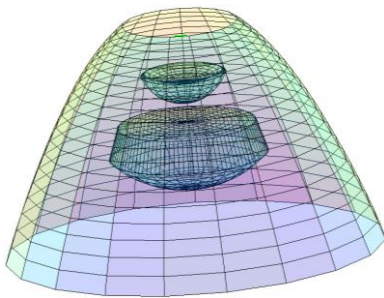


Fig. 5. The three-dimensional schematic diagram of the collimating system

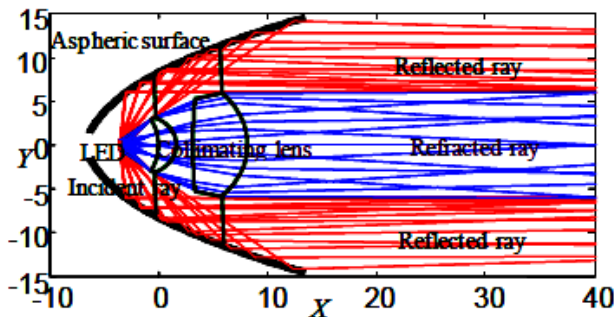


Fig. 6. The 2D simulation of LED lights passing through the collimator

Fig. 7 shows the 3D optical path simulation of LED lights within the propagation distance of 500 mm, in Fig. 7, the green lines represent the light rays refracted out of the

middle lenses, and the red lines represent the light ray reflected from the reflector. The divergence angles of the refracted light rays are larger than the reflected light rays. All the light rays fall within a semi-divergence-angle of 4.6 degree, which means an optical efficiency will reach 100% within 4.6 degree without the Fresnel loss and the optical absorption of materials.

Fig. 8 shows several special intersection points, among them, (12.49, 14.21) and (-3.02, 5.98) are points having the maximum y value and the minimum y value on the reflecting surface respectively, these two coordinates together with the central coordinate of LED determine the functional vertical and horizontal size of the collimator system. The size in the x direction is 15.99 (3.5+12.49) mm, and the size in the y direction is 28.42 (2×14.21) mm. Coordinates of the maximum incident ray height on four surface are (-0.70, 2.90), (-0.41, 3.15), (3.31, 5.12) and (5.83, 5.88), respectively. These four coordinates determine the height of front surface and rear surface of the meniscus lens and a biconvex lens.



Fig. 7. The simulation of light path at long distances after the collimator system

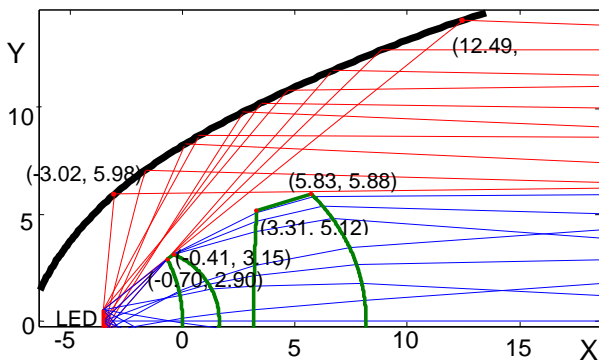


Fig. 8. Several special intersection points between light rays and the collimator system

#### 4.3. The simulation of light intensity distribution on a plane perpendicular to the optical axis

In Fig. 4, let  $m_1=41$ ,  $m_2=81$ , so altogether 6306369 light rays are traced. Each ray carries the energy according to Lambert's law. By means of statistics of positions at which these rays arrive, a shape of outgoing light spot which stands for the light intensity distribution on the vertical axis plane can be drawn. The change of spot shape with the exit distance is shown as in Fig. 9, and numbers in Fig. 9 are the x-coordinate values.

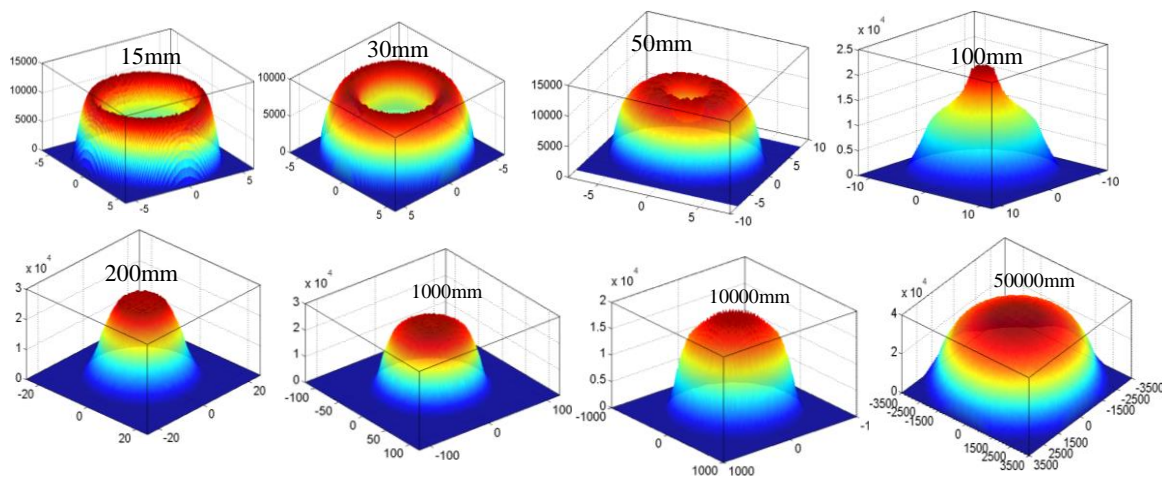


Fig. 9. The computer simulation of light intensity distribution on the vertical axis plane at different positions

Fig. 10 is a group of intensity charts corresponding to Fig. 9 and simulated in LightTools Illumination Design Software. It can be seen that Fig. 10 and Fig. 9 are almost identical, which signifies the correctness of design processes in this paper. Because the experiment in following section is conducted with only the collimating lenses in the middle of the system, for comparison, the simulations of light intensity distribution are performed just for the collimating lenses

Fig. 9 and Fig. 10 show that the intensity at the spot periphery is higher than the central area for  $x < 50$  mm, and spots are crater-shaped. At  $x = 100$  mm, the crater disappeared into the bright center of a spot. The bright

center expands with increasing  $x$ , the whole spot evolves into such forms whose center is slightly stronger in intensity than around spot. The collimators which produce such light intensity distribution can be applied to flashlights, head lamps, etc

Fig. 11 is the simulation of light intensity distribution on the vertical axis plane at  $x = 5000$  mm when we take one-quarter, two-quarters, three-quarters and four-quarters of a round LED. The shape of exit light spot is similar to the shape of light source. While there is a defect in the shape of light source, there is also the same defect in the shape of exit light spot. This shows that the spot in this case is the image of the light source.

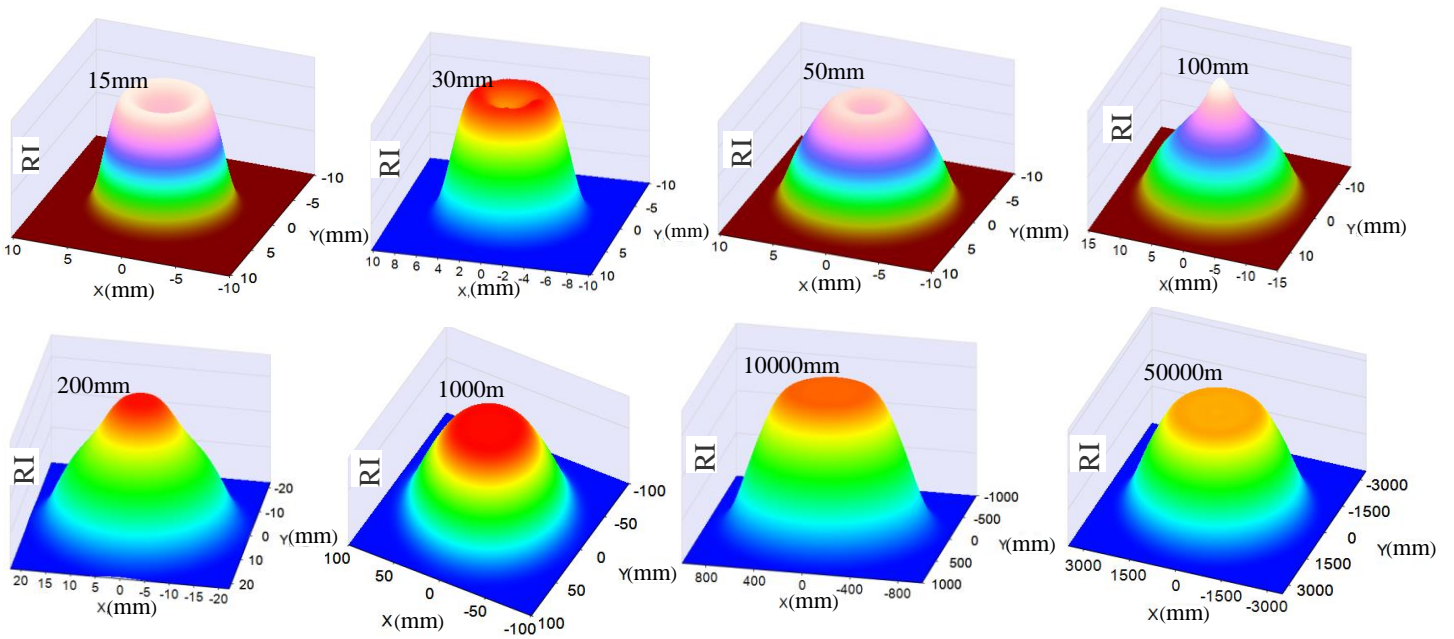


Fig. 10. Lighttools simulations of light intensity distribution on the vertical axis plane

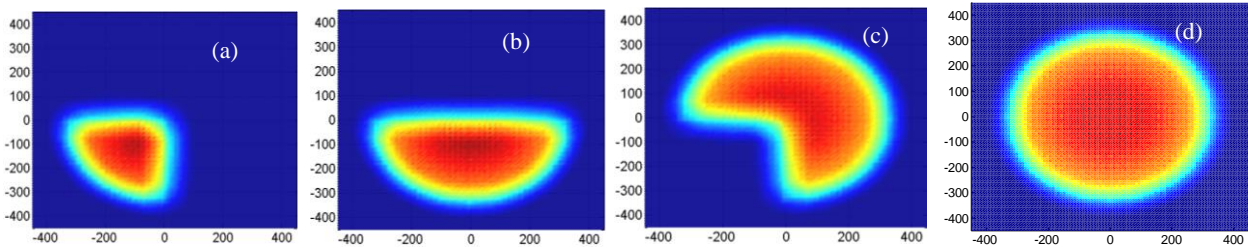


Fig. 11. The computer simulations of light distribution on the vertical axis plane at  $x=5000$  mm, (a) one-quarter of round LED, (b) two-quarters of round LED, (c) three-quarters of round LED, (d) the whole round LED

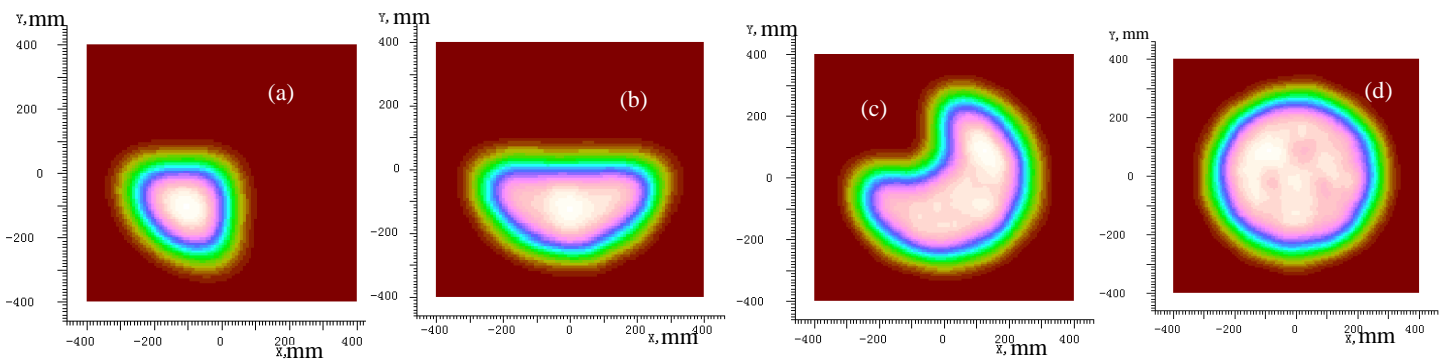


Fig. 12. The lighttools simulations of light distribution on the vertical axis plane at  $x=5000$  mm, (a) one-quarter of round LED, (b) two-quarters of round LED, (c) three-quarters of round LED, (d) the whole round LED

Fig. 12 shows the lighttools simulations of light intensity distribution corresponding to Fig. 11. Fig. 12 is good agreement with Fig. 11, which represents the appropriateness of research design by this method.

## 5. Experiment

Fig. 13 shows the photos of the meniscus and bi-convex lenses. The lens material is K9 glass (Manufactured by Changchun Jia Fu Opto-Electronic Co., Ltd., China). Since the reflecting surface outside the

collimator system is aspheric, its cost will be high. The divergence angle of the emitted light is mainly caused by the collimating lenses, so we only produced the collimating lenses, and then carried out the experiment for the purpose of verifying the collimation effect of the collimating lenses.



Fig. 13. Photos of the meniscus and the bi-convex lenses, the smaller one (diameter  $\sim 6$  mm) is the meniscus lens and the bigger one is the bi-convex lens (diameter  $\sim 12$  mm)

Fig. 14 shows the photos of the experimental device and the simple method for measuring the spot size. The spot diameter can be read from the ruler at the spot, and the divergence angle of the beam can be calculated.

A LED light source emits green light having the center wavelength 520 nm, the refractive index of K9 glass  $n = 1.5168$  at wavelength 520 nm. Fig. 15(a) shows the photo of the spot on the vertical axis plane at  $x \approx 30$  mm, it can be seen that the picture is crater-shaped and its middle region is slightly darker than its surrounding region. Due to the diffuse scattering of light on the screen, the shape of the crater is not very clear, but distinguishable. This spot photo is well consistent with Fig. 9.

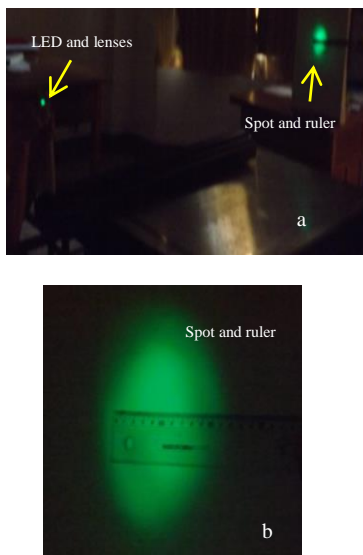


Fig. 14. The photos of the experimental device and the measurement of the spot size. (a) Photo of the whole lightpath; (b) Spot measuring

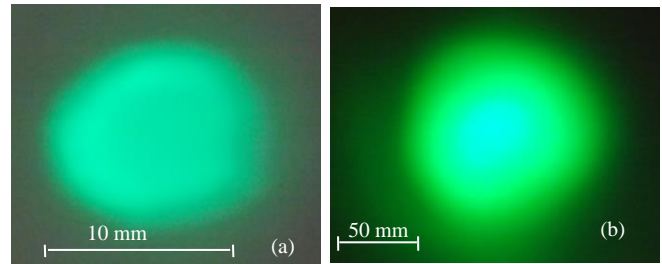


Fig. 15. Experimental results (a) The light spot on the vertical plane at  $x \approx 30$  mm; (b) The light spot on the vertical plane at  $x = 1000$  mm

Fig. 15 (b) shows the photo of the light spot on the vertical axis plane at  $x = 1000$  mm, the maximum half divergence angle  $4.6^\circ$  of exit light rays can be calculated from Fig. 15 (b), and this value well coincides with the theoretical result. It can also be seen from Fig. 15 (b) that the light intensity is strongest in the spot's middle region and weaker on the edge, which also well coincides with its computer simulation.

The shape of the spot in Fig. 15 is not strictly circular. We can deduce from the image simulation in Fig. 11 and Fig. 12 that the LED source itself is not strictly circular. It has been assumed that the LED source is a Lambert emitter when we simulate the light distribution. Therefore the consistency of experimental and simulation results confirms this assumption.

## 6. Conclusions

The paper employed the CLPSO algorithm to design a collimator system for planar light sources, and the implementation procedure is described in details. By using this method, an optical system with low energy loss and high collimation for the round LED of 1.0 mm diameter has been designed, and its light emission caliber is 30mm. If Fresnel losses, material absorptions and light shining on the interface are not taken into account, the computer simulation results demonstrated that this system can achieve a collimated beam with an optical efficiency of 100 % under a divergence angle of  $\pm 4.6$  deg based on a 1.0 mm diameter round LED chip. The experiment on the collimating lenses in the middle of the system shows that experimental results are consistent with the simulation, which verifies the correctness of design results and the design method.

Compared with the existing design method in literatures, the method in this paper is straightforward in surface light sources, more intuitive and clear, and the accurate equations of reflective or refractive surface can be directly achieved, which avoids the trouble of constructing free-form surfaces from discrete points, also eliminates an intensity distribution shift on the target surface caused by fitting errors in the process of fitting free-form surfaces from discrete points. This method can be used to design various LED luminaires for general or

specific illumination applications.

### Acknowledgements

Financial support from SDUT & Zibo City Integration Development Project (No. 2017ZBXC021) and Shandong province reform project on undergraduate education (No. M2018X220).

### References

- [1] L. Wang, K. Qian, Y. Luo, *Appl. Opt.* **46**, 3716 (2008).
- [2] F. R. Fournier, W. J. Cassarly, J. P. Rolland, *Opt. Express* **18**, 5295 (2010).
- [3] J.-J. Chen, C.-T. Lin, *Opt. Eng.* **49**, 093001 (2010).
- [4] W. Zhang, Q. Liu, H. Gao, F. Yu, *Opt. Eng.* **49**(6), 063003 (2010).
- [5] Y. Ding, X. Liu, Z. R. Zheng, P. F. Gu, *Opt. Express* **16**, 12958 (2008).
- [6] H. Ries, J. Muschaweck, *J. Opt. Soc. Am. A* **19**, 590 (2002).
- [7] G. Wang, L. Wang, L. Li, D. Wang, Y. Zhang, *Appl. Opt.* **50**, 4031 (2011).
- [8] J. J. Chen, T.Y. Wang, K. L. Huang, T. S. Liu, M. D. Tsai, Ch. T. Lin, *Opt. Express* **20**, 10984 (2012).
- [9] J. Mackey, *Astron. Astrophys.* **539**, A147 (2012).
- [10] M. B. Hulin, J. Hanika, W. Heidrich, *Comput. Graph. Forum* **31**, 1375 (2012).
- [11] Y. Ding, Zh. R. Zheng, P. F. Gu, *Acta Photonica Sinica* **38**, 1486 (2009).
- [12] G. Wang, L. Wang, L. Li, D. Wang, Y. Zhang, *Appl. Opt.* **50**, 4031 (2011).
- [13] J. J. Liang, A. K. Qin, P. N. Suganthan, S. Baskar, *IEEE T. Evolut. Comput.* **10**, 281 (2006).
- [14] Y. Shi, R. C. Eberhart, *Proc. IEEE Congr. Evol. Comput.* 69 (1998).
- [15] A. Y. Abdelaziz, F. M. Mohammed, S. F. Mekhamer, M. A. L. Badr, *Electric Power Systems Research* **79**(11), 1521 (2009).
- [16] Andi Muhammad Ilyas, M. Natsir Rahman, *Telkomnika* **10**(3), 459 (2012).

---

\*Corresponding author: zfqinh@163.com